JOURNAL OF GUIDANCE, CONTROL, AND DYNAMICS
Vol. 16, No. 2, March-April 1993

Robust Flight-Path Control System Design with Multiple-Delay Model Approach

Yoshikazu Miyazawa*
National Aerospace Laboratory, Chofu, Tokyo, Japan

Robust control system design with a multiple-delay model approach is applied to a flight-path and velocity control problem. The approach is based on concepts of multiple models, linear quadratic regulator, and proportional output feedback. Multiple-delay models are used to represent uncertain dynamics in the high-frequency range. The performance index is defined with a quadratic function presenting the design goal in a natural manner, and the control law is obtained by minimizing the performance index. The control law obtained by the multiple-delay model approach is robust against unstructured uncertainty and is a natural extension of the linear quadratic regulator to increase the robustness without performing complicated adjustments of the quadratic performance-index weighting matrices. A flight-path and velocity control problem for a lightweight transport is studied to examine feasibility of the approach. Crossover frequency and phase margin, frequency-response matrix singular values, control performance change due to the parameters' variation, and command input time responses including nonlinear dynamics effects are studied to demonstrate the robustness of the control laws. Numerical results show the feasibility and usefulness of the approach.

Introduction

CONTROL system robustness against uncertain and/or changing dynamics is a major control engineering research area. Analytical methods based on both the frequency response and the H_∞ criteria have especially been developed and also extensively applied to practical flight-control problems. The present study incorporates the multiple-model (MM) approach for the same objectives, i.e., control systems should be designed to have a necessary and sufficient margin against unavoidable uncertainties/changes in the given mathematical model, while simultaneously maximizing control performance.[1-6]

In robust control system designs, representation of the uncertainty is important. One of the biggest advantages of using the MM approach is that it can directly and easily represent uncertainties. This approach provides a straightforward method for control engineers to construct mathematical models of uncertain dynamics, e.g., grid points selected to represent uncertain and/or changing parameters can be used as design models. Implementing a user-friendly computer-aided design environment and efficient computational optimization algorithms will help to enhance the MM approach to be a useful analytical design technique. In practical control system designs, feedback control frequency bandwidths are frequently more important to obtain control system robustness than parameter uncertainty,[7] with most MM approaches failing to explicitly treat this condition. The present study proposes "a multiple-delay model (MDM) approach" to incorporate the necessary margins against uncertainty in the high-frequency range, while simultaneously maximizing control performance.[8,9] Generally, the phase of frequency response is quite uncertain in the high-frequency range, this being the reason why practical applications of high gain feedback control are largely unsuccessful. In the proposed MDM approach, high-frequency uncertainty is represented with uncertain delay models. Since the uncertain delay naturally suppresses the amount of feedback gain, the approach can introduce the feedback gain upper limit even if the control cost is not taken into account, i.e., in the so-called cheapest control case.

Another advantage of using the MDM approach is that it considers the control performance and can minimize the performance index similar to a standard linear quadratic regulator (LQR), therefore preventing too conservative results from being obtained. In addition, it also includes simple and practical control laws. Since the performance index is minimized by parameter optimization, the feedback control structure can arbitrarily be defined. When full-state feedback control is considered as the most complex control, then partially closed-loop cases can be examined by comparing the minimized performance-index values. The delay model's state variable introduced with this approach is not directly accessible and subsequently not included in the feedback states. One disadvantage is related to this characteristic, i.e., predetermined control structure. Prior to the numerical calculations, the approach does not furnish information on how the loop should be closed, on what kind of dynamic compensator is necessary, or if a feedback gain exists that can simultaneously stabilize all models. Therefore, the approach might need some sense of an engineering control system design like classical synthesis methods. Even though these problems have led to new analytical methods such as the H_∞ approach,[10] studies must be conducted using various techniques that enable the optimal control laws to be introduced into practical control system design.

In the present paper, a longitudinal flight-path control problem is discussed that utilizes the proposed MDM approach. A numerical example for a lightweight transport was examined to demonstrate feasibility of this approach. Another example for a powered STOL (Short Takeoff and Landing) aircraft was studied in Ref. 9. With the MDM approach, control laws can be obtained with only a few design parameters, e.g., the delay times for each control input. The resulting control laws were found to be suitable for practical implementation and subsequently showed the usefulness of this approach.

Landing Approach Longitudinal Flight-Path Control

Aircraft flight paths must be precisely controlled during landing approach. This typical flight control problem was examined using the MDM approach. The analysis was conducted using an equation for point-mass longitudinal motion, where the aircraft dynamics are defined as

$$\frac{dx}{dt} = Ax(t) + B\delta(t) \tag{1}$$

Presented as Paper 91-2671 at the AIAA Guidance, Navigation, and Control Conference, New Orleans, LA, Aug. 12-14, 1991; received Oct. 21, 1991; revision received May 11, 1992; accepted for publication May 29, 1992.

*Head, Flight Analysis Section, 6-13-1 Osawa, Mitaka. Member AIAA.

$$A = \begin{bmatrix} \kappa(-2C_D - C_{D_u}) & -g/U_0 + \kappa C_{D_\alpha} & 0 \\ \kappa(2C_L + C_{L_u}) & g/U_0 \sin\gamma_0 - \kappa C_{L_\alpha} & 0 \\ 0 & 1 & 0 \end{bmatrix}$$

$$B = \kappa U_0 \begin{bmatrix} -C_{D_\alpha} & \cos\theta_T \\ C_{L_\alpha} & \sin\theta_T \\ 0 & 0 \end{bmatrix}$$

where $x^T = [u, \mathrm{d}h/\mathrm{d}t, h]$ and $\delta^T = [\theta, C_T]$ are, respectively, the state and control vectors. u is the true airspeed (m/s), $\mathrm{d}h/\mathrm{d}t$ the vertical velocity (m/s), h the glide path vertical deviation (m), θ the pitch attitude (rad), and C_T the thrust coefficient. All these variables, except for h, are deviations from the equilibrium condition nominal values. Parameters are defined as $g = 9.80$ (m/s^2) gravity acceleration, γ_0 nominal glide path angle (rad), $\kappa = \frac{1}{2}\rho U_0 S/m$ (1/s), where ρ is air density (kg/m^3), U_0 nominal true airspeed (m/s), S wing area (m^2), and m mass (kg). θ_T (rad) is the thrust vector inclination angle. Aerodynamic coefficients C_L, C_D, and aerodynamic derivatives C_{L_α}, C_{D_α}, C_{L_u}, C_{D_u} are evaluated at the equilibrium point. Equation (1) was derived using the assumptions that $\cos(\gamma_0) = 1$ and $\sin(\theta) = \theta$.

The equation of point-mass approximation uses only a static aerodynamic force, and its accuracy is limited to the low frequency. Furthermore, an elevator-controlled pitch attitude, or inner-loop control, is assumed, and the pitch attitude is considered as a control input. In general, the pitch attitude can exactly track the command in a certain frequency bandwidth, although this is not justified in the high-frequency range. However, these possible inconsistencies can be included using the MDM approach.

Figure 1 shows the block diagram used for the MDM control system. The equation of point-mass longitudinal motion is presented by Eq. (1), and uncertainty/unmodeled dynamics are represented by the uncertain delay models, $\phi_\theta(s)$, $\phi_T(s)$. The following design models were selected:

$$\phi_\theta(s) = k_\theta \frac{1 - T_\theta s/2}{1 + T_\theta s/2}, \qquad k_\theta = 1$$

$$T_{\theta_1} = T_{\theta_3} = 0, \qquad T_{\theta_2} = T_{\theta_4} = T_{\theta_0} \tag{2a}$$

$$\phi_T(s) = k_T \frac{1 - T_T s/2}{1 + T_T s/2}, \qquad k_T = 1$$

$$T_{T_1} = T_{T_2} = 0, \qquad T_{T_3} = T_{T_4} = T_{T_0} \tag{2b}$$

Subscripts 1–4 correspond to four multiple-delay models, with each model representing the uncertainty in each control input response, i.e., transfer function ϕ_θ is from the pitch attitude command to the actual pitch attitude, whereas transfer function ϕ_T is from the thrust command to the actual thrust. Two delay models are used for representing the high-frequency uncertainty of each control input response, where one has no delay and the other has approximately a $T_{\theta_0}(T_{T_0})$ second delay. The $T_{\theta_0}(T_{T_0})$ second delay model has a phase lag ranging from 0 deg at low frequencies to 180 deg at high frequencies, having a 90-deg phase lag at frequency $2/{}_{\theta_0}(2/T_{T_0})$ (rad/s). As it will be demonstrated in later numerical examples, this frequency can approximately give the control frequency bandwidth, therefore it can be called the boundary frequency. The gains of delay model frequency response, Eqs. (2), are constantly unit for all frequencies.

The control system design was performed by minimizing an appropriately defined quadratic performance index, i.e., the flight-path control design goal for a landing approach condition is that vertical deviation from the glide path and true airspeed error from the nominal value should be minimized, thus the following performance index was defined to realize this goal.

$$J = \sum_{i=1}^{4} p_i J_i$$

$$J_i = E\left[\int_0^\infty \left\{\left[h_i(t) - h_c\right]/h_0\right\}^2 + r\left\{\left[u_i(t) - u_c\right]/u_0\right\}^2 \mathrm{d}t\right] \tag{3}$$

The performance index is a weighted sum of performance indices for each model, with subscript i denoting the variable of the ith delay model system and p_i (>0, $\Sigma p_i = 1$) being either the probability of the ith model or an adjustable weighting parameter. In the following numerical example, four models are simply equally weighted, i.e., $p_i = \frac{1}{4}$. $E[\ ]$ denotes an average that corresponds to the randomly distributed initial condition. Each model's performance index is introduced from a servo problem for the two outputs of path deviation $h(t)$ and true airspeed $u(t)$, where h_c and u_c are constant commands presenting arbitrary set points for each output. A weighting parameter r presents the balance between the velocity error and the flight-path deviation. In the present paper, $r = 1$ is simply selected, meaning that these two errors are equally weighted in the quadratic performance index. As for h_0 and u_0, they must be appropriately defined to normalize their corresponding physical variables.[11] It is reasonable to select these parameters having the same energy, i.e., since the energy deviation can be approximated as $m(gh + U_0 u)$, where U_0 is the nominal true airspeed, u_0 is defined as $u_0 = gh_0/U_0$. The two control variables, pitch attitude and thrust, are normally able to control the steady state of the two outputs, thus the infinite time integral of the performance index can be a finite value. Since the control cost is not taken into account, it becomes the so-called cheapest control problem.

The initial condition influences the control law in the MDM approach, hence it must be appropriately given to represent each variable's probable deviations. This is done by simply defining that all states including delay-model states are equal to zero, and that the two command inputs are random variables of zero mean with the appropriately given variances, i.e.,

$$E\left[x(0)x^T(0)\right] = 0$$

$$E\left[(h_c/h_0)^2\right] = 1, \quad E\left[(u_c/u_0)^2\right] = 1, \quad E\left[h_c u_c\right] = 0 \tag{4}$$

The control law is assumed to be an output feedback having a constant multivariable gain matrix.

$$\delta_i^*(t) = K\xi_i(t)$$

$$\delta_i^{*T} = \left[\theta_i^*(t), C_{T_i}^*(t)\right]$$

$$\xi_i^T = \left\{\int_0^t \left[u_i(\tau) - u_c\right] \mathrm{d}\tau, \int_0^t \left[h_i(\tau) - h_c\right] \mathrm{d}\tau, u_i(t), h_i(t), \frac{\mathrm{d}h_i}{\mathrm{d}t}\right\} \tag{5}$$

The output consists of both aircraft dynamics states $[u, \mathrm{d}h/\mathrm{d}t, h]$ and the time integrals of the two output errors $[u - u_c, h - h_c]$. The integral feedback is necessary to compensate for output bias errors. The feedback control structure, Eq. (5), is derived from a standard LQR servo problem.[12] Since this full output feedback control is not necessarily required in practical control design and suboptimal partially closed-loop

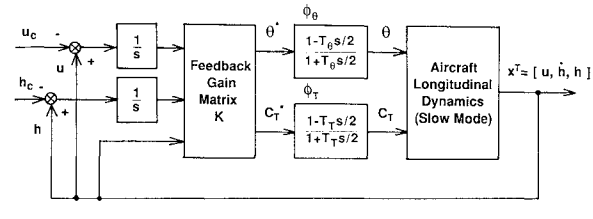

Fig. 1 Block diagram of a longitudinal flight-path control system.

Table 1 Multiple-delay models

Model, i	1	2	3	4
T_θ, s	0	2	0	2
T_T, s	0	0	2	2

Table 2 Feedback gains

Control law 1 (output feedback):

$$K = \begin{bmatrix} 0.00739 & -0.00503 & 0.00644 & -0.01043 & -0.01795 \\ -0.01615 & -0.00410 & -0.07920 & -0.01769 & -0.01726 \end{bmatrix}$$

Control law 2 ($h \rightarrow \theta$; u, $h \rightarrow C_T$):

$$K = \begin{bmatrix} 0 & -0.00506 & 0 & -0.03228 & -0.01890 \\ -0.01877 & -0.00462 & -0.07847 & -0.02305 & -0.01865 \end{bmatrix}$$

Control law 3 ($h \rightarrow \theta$; $u \rightarrow C_T$):

$$K = \begin{bmatrix} 0 & -0.00371 & 0 & -0.03760 & -0.01753 \\ -0.01833 & 0 & -0.09296 & 0 & 0 \end{bmatrix}$$

Control law 4 ($h \rightarrow \theta$; $u \rightarrow C_T$):

$$K = \begin{bmatrix} 0 & -0.00158 & 0 & -0.02464 & -0.02294 \\ -0.00098 & 0 & -0.02062 & 0 & 0 \end{bmatrix}$$

Table 3 Performance index, crossover frequency, and phase margin

Control law	P.I.	ω_θ, rad/s/PM_θ, deg	w_T, rad/s/PM_T, deg
1	7.795	0.96/97	0.63/73
2	8.089	0.92/98	0.64/68
3	9.171	1.22/104	0.77/78
4	28.43	0.96/89	0.17/80

controls often give similar performances, a structured control law needs to be considered. For example, the following constraint is posed on the feedback gain matrix.

$$K = \begin{bmatrix} 0 & X & 0 & X & X \\ X & 0 & X & 0 & 0 \end{bmatrix} \tag{6}$$

where the zeros correspond to loops that are not closed, and X denotes a nonzero element that can be optimized in a structured control law.

The feedback gain is then obtained by minimizing the performance index, Eq. (3), under the initial conditions, Eq. (4). The optimal control law subsequently depends on the weighting parameters u_0, h_0, r, p_i, and the initial conditions; thus these variables should be appropriately given. The MDM approach incorporates a rule in which the performance index directly represents the design goal and those design parameters are supplied using the sound engineering judgments of control designers.

Concerning the parameter-optimization computational algorithm for the MDM approach, a previously reported penalty-function method[6] and the quasi-Newton method were used. The penalty-function method is suitable when there is no obvious feedback gain that can simultaneously stabilize all of the multiple models, although this method requires significant computational time in order to obtain desired accuracy, hence the quasi-Newton method was used to increase final accuracy.

Design Example

A design example was numerically calculated for a twin turboprop lightweight transport, which is being used as a research airplane by the National Aerospace Laboratory (NAL), Japan. Equation (1) parameters are given as $C_L = 1.333$, $C_D = 0.1383$, $C_{L_\alpha} = 5$, $C_{D_\alpha} = 0.5937$, $C_{L_u} = 0$, $C_{D_u} = 0.0685$, $\gamma_0 = -3$ deg, $\theta_T = 11.3$ deg, $U_0 = 45$ m/s, and $1/\kappa = 6.122$ s. These values were estimated for a typical landing approach condition, i.e., $m = 5400$ kg, 20 deg flap down, and landing gear down.[13] Aerodynamic derivative C_{D_u} is due to the propeller-driven thrust. Since two delay times were used for the two control inputs, a total of four models was considered as listed in Table 1. These uncertain delay time values were not rigorously derived from actual dynamics, but they were instead chosen for this numerical example, with the selected multiple models incorporating equal delay times ranging from 0 to 2 s. Since the thrust and pitch attitude control frequency bandwidths are considered comparable, the same delay models were used for both inputs.

Control Laws and Performance Indices

The optimal control laws were obtained by minimizing the performance index, Eq. (3), for the four control gain structures. The resulting optimal feedback gains and performance indices are listed in Tables 2 and 3. Control law 1 uses full output feedback and gave the best control performance among the four control gain structures. Control law 2 uses an open loop from velocity to pitch attitude, and subsequently gave a very similar performance index to that of control law 1. Control law 3 is a standard autopilot structure used in a landing approach mode, i.e., path-deviation control with the pitch attitude and airspeed control with the autothrottle. Control law 3 gave a fair performance index, thus showing good correlation with practical designs. Control law 4 is obtained using different uncertain delay models and it will be discussed in the section "Different Control Frequency Bandwidths."

Table 3 also gives crossover frequencies and phase margins, which were obtained by breaking a loop at a specific control input point while maintaining the other loop closed under the assumption of no delay time, i.e., $T_\theta = T_T = 0$. Crossover frequencies range from 0.63 to 1.22 rad/s, where the given delay models' boundary frequencies are both 1 rad/s ($= 2/T_{\theta_0}$, or $2/T_{T_0}$). It should be noted that the obtained crossover frequencies are comparable with the given boundary frequency, and in most cases the crossover frequency is slightly lower than the boundary frequency. Roughly speaking, by using the proposed MDM and the cheapest control, the boundary frequency gives upper crossover frequency limit for each control input. The obtained phase margins range from 60 to 104 deg, being comparable or greater than those obtained by a standard LQR. These values clearly indicate the robustness of the control laws obtained using the MDM approach.

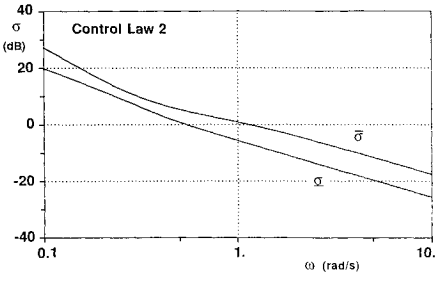

Fig. 2a Singular values of frequency-response matrix (control law 2).

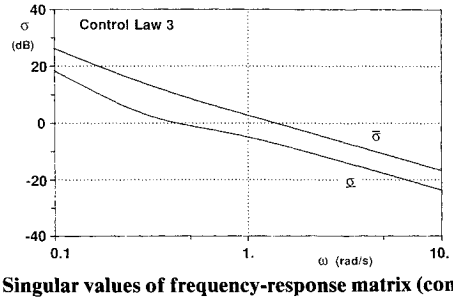

Fig. 2b Singular values of frequency-response matrix (control law 3).

Singular values of the frequency-response matrix were examined for each control law. Figures 2a and 2b, respectively, show control laws 2 and 3, where break points are located at the control inputs and no delay time is assumed. Since two control inputs were used, the two curves indicate the maximum and minimum singular values. The boundary frequencies considered for each input are equally 1 rad/s. The maximum singular value is small in the high-frequency range and indicates sufficient robustness against unstructured uncertainty. On the other hand, the minimum singular value is large enough in the low-frequency range and indicates adequate disturbance-rejection characteristics. The control law 1 full output feedback results (data not shown) are quite similar to those of control law 2. Figures 2a and 2b show that control laws 1 and 2 are only slightly better than control law 3 in both the high- and low-frequency ranges. Since control law 3 can be considered as a standard structure for practical control and gives fairly good control performance, it will be discussed in the following sections, unless otherwise specifically cited.

Robustness Against Parameter Changes

Figure 3a shows the performance-index contour with respect to the delay times for each control input. Four design points are explicitly considered in the MDM approach. The nominal delay times T_θ and T_T were set a 1 s, and the performance-index value is normalized with the one occurring at the nominal point. Although the control law is introduced from only four design points, where the closed-loop stability is guaranteed, the obtained performance-index contours are nearly level over the design region from 0 to 2 s delay time. This performance-contour chart can be considered as a measure of the control system robustness against unstructured high-frequency uncertainty.

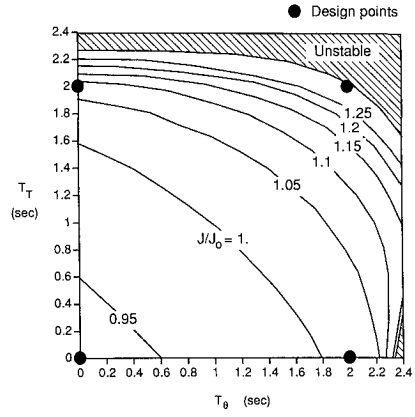

Fig. 3a Performance contour with respect to delay times (control law 3).

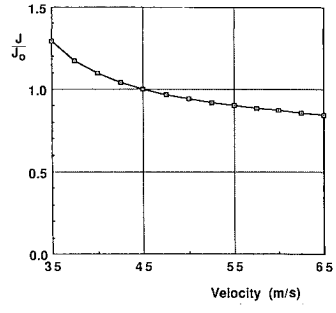

Fig. 3b Robustness with respect to nominal airspeed change (control law 3).

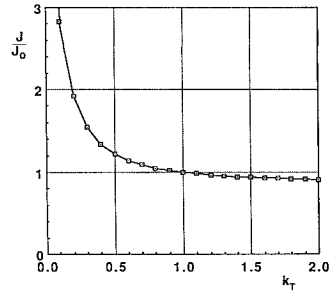

Fig. 3c Robustness with respect to thrust gain change (control law 3).

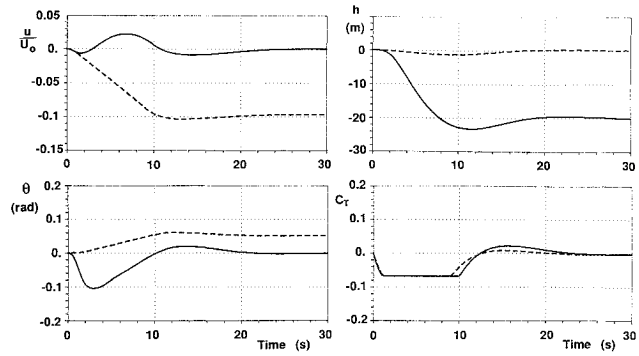

Fig. 4a Command input responses obtained with control law 2 (——: vertical deviation command; - - - -: airspeed command).

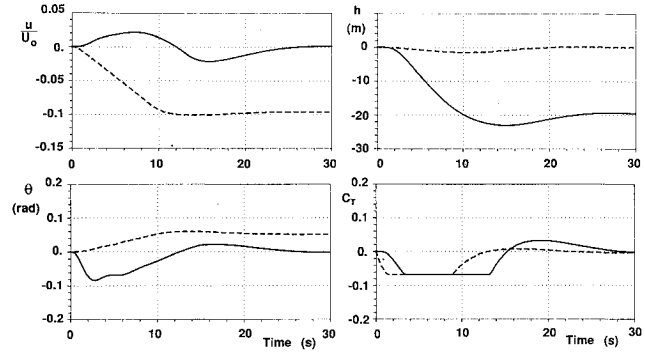

Fig. 4b Command input responses obtained with control law 3 (——: vertical deviation command; - - - -: airspeed command).

In flight-control system designs, both structured and unstructured uncertainty must be considered. The MDM approach is very flexible, and easily enables structured uncertainty to be included by adding other appropriate models, although here only unstructured high-frequency uncertainty is considered, whereas parameter uncertainty and/or parameter change of the aircraft dynamics are not explicitly considered. In many cases, however, small parameter changes do not have a large influence on either control performance or the optimal control law, especially when the feedback gain is fairly high. With the MDM approach, the feedback control is designed to be tight as much as possible to the level where it does not degrade the regulator performance due to the high-frequency uncertainty, thus it is also robust against parameter changes. To demonstrate this feature, the influence of parameter changes was examined, with both uncertain delay times being fixed at 1 s, i.e., the average of the two delay times used in the multiple models.

Figure 3b shows the performance change with respect to the nominal velocity change, where the control law was designed for 45 m/s. Trimmed lift coefficients were calculated for each nominal velocity, and aerodynamic derivatives were estimated from the drag polar curve. The performance-index value is normalized by the one occurring at the design point (45 m/s). Although the designed flight velocity (45 m/s) is almost at a boundary of the front and back sides of the drag polar curve, the control performance velocity dependence is not significant. Since the autothrottle is highly active, the nominal velocity change effect on the lift/drag ratio (L/D) becomes small. The autothrottle is therefore important, and it would be expected

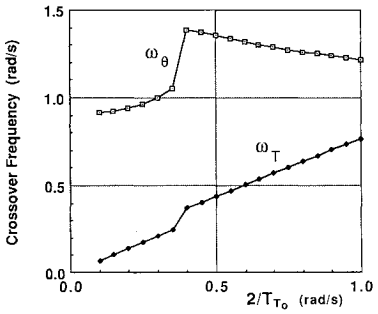

Fig. 5a Crossover frequency with respect to thrust control delay time.

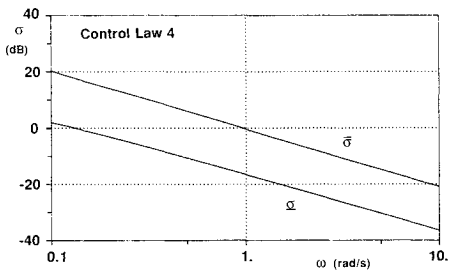

Fig. 5b Singular values of frequency response matrix (control law 4).

that the thrust amount generated by the command has significant influence on the control performance. Figure 3c shows the effect of varying k_T in Eq. (2), where the design thrust gain k_T is 1. The control-performance curve is level around the design point, although the performance degradation becomes significant when the thrust gain is less than 20%.

Robustness Against Nonlinear Dynamics

The motivation behind the proposed approach is to incorporate high-frequency uncertainty, sources of which are, for example, flexible modes, actuator nonlinear dynamics, sensor dynamics, digital signal processing time delays, and filters. Some of these uncertainties can be quantized and modeled in the aircraft dynamics equation, although most cannot be precisely modeled because their dynamics are nonlinear to some extent. Pitch rate and acceleration generated by the elevator control would reach saturation due to the limited elevator control power or the limited control authority. The thrust and its rate are limited as well. Phase lags due to these nonlinear effects are included in the MDM approach. Numerical simulation was conducted in order to verify the closed-loop system robustness against such nonlinear effects.

Figures 4a and 4b, respectively, show the control systems' response with control laws 2 and 3. Two cases of command inputs are considered, i.e., ($h_c = -h_0$, $u_c = 0$) and ($h_c = 0$, $u_c = -u_0$), where $h_0 = 20$ m and $u_0/U_0 = 0.0968$. Constraints of $|\theta| < 0.1$ rad, $|C_T| < 0.0685$, and $|dC_T/dt| < 0.1$, are posed, and pitch attitude generation is assumed to be realized with a second-order system having an undamped natural frequency of 2 rad/s and damping coefficient of 0.7. Since the path-deviation and velocity-error responses of the two command cases are explicitly considered with the performance index, Eq. (3), and the initial condition, Eq. (4), favorable responses can be naturally expected. On the whole, the obtained responses are appropriate in spite of the nonlinear dynamics effect. Moderate rise times are mainly due to the modeled uncertain delays or the limited control frequency bandwidths. Although there are overshoots in the path-deviation command responses, they could be accepted as a compromise between no-bias error condition and uncertain delays. Comparing control laws 2 and 3, both control laws give similar response in the velocity command case, but in the path-deviation command case, control law 2 gives slightly better response than control law 3. With these control laws, the thrust controls the kinetic energy and the pitch attitude controls the energy distribution between the path deviation and the velocity change, and control law 2 realizes this more efficiently than control law 3.

Different Control Frequency Bandwidths

One of the MDM approach merits is that it can easily adjust the frequency bandwidth at any point in the closed-loop system. As an example, the thrust control frequency bandwidth design was studied. The control law 3's feedback gain from airspeed to thrust is large, when it is compared with a pilot's handling. In case of pilot's manual control, the airspeed cannot be continuously checked, thus an adequate margin might be necessary in the loop from airspeed to thrust. To simulate this control, the thrust input delay time T_{T_0} was increased, and the optimal control for control law 3 type structure was calculated for each delay time. Figure 5a shows each loop's crossover frequencies. Although the thrust loop's crossover frequency proportionally decreases with decreases in the boundary frequency $2/T_{T_0}$, the pitch loop's crossover frequency remains near its boundary frequency $2/T_{\theta_0}$ (= 1 rad/s). The control law obtained for $T_{T_0} = 8$ s is listed in Table 1 as control law 4. It should be noted that the thrust loop gains are significantly decreased to increase the thrust loop stability margin. Figure 5b shows the singular values of the frequency response, the definition of which is the same as it was in Figs. 2a and 2b. Compared with Fig. 2b, the difference between the maximum and minimum singular values is larger than control law 3. Since the control frequency bandwidths were designed to be different for the two control inputs, this result is considered reasonable.

Concluding Remarks

A longitudinal flight-path and velocity-control problem was studied using a robust control system design method, i.e., the multiple-delay model approach. Transport-type aircraft landing approach flight control was selected as a numerical example, and the control laws obtained with the approach were examined from various aspects, such as frequency-response matrix singular values, influence of important parameter changes, and effects of nonlinear dynamics. Results show that the obtained control laws are satisfactory regarding control performance and robustness. Since the control law minimizes an appropriately defined quadratic performance index, it does not give excessively conservative control performance. The frequency bandwidth at any point in the closed-loop system can be efficiently adjusted with the multiple-delay model approach in conjunction with the so-called cheapest control. The control law can be derived with only a few design parameters, such as delay times. Therefore, the control system design can be conducted in a straightforward manner or with limited trial and error. It is expected that this approach has high potential for application to various kinds of flight control problems.

References

[1]Ackermann, J., "Multi-Model Approaches to Robust Control System Design," *Lecture Notes in Control and Information Sciences,* Vol. 70, Springer-Verlag, Berlin, Germany, 1985, pp. 108–130.

[2]Vinkler, A. P., Wood, L. J., Ly, U., and Cannon, R. H., Jr., "Minimum Expected Cost Control of a Remotely Piloted Vehicle," *Journal of Guidance and Control,* Vol. 3, No. 6, 1980, pp. 517–522.

[3]Ly, U., "A Design Algorithm for Robust Low-Order Controller," Ph.D. Dissertation, Dept. of Aeronautics and Astronautics, Stanford Univ., Stanford, CA, 1982.

[4]Ashkenazi, A., and Bryson, A. E., Jr., "Control Logic for Parameter Insensitivity and Disturbance Attenuation," *Journal of Guidance, Control, and Dynamics,* Vol. 5, No. 4, 1982, pp. 383–388.

[5]Gangsaas, D., Bruce, K. R., Blight, J. D., and Ly, U., "Application of Modern Synthesis to Aircraft Control: Three Case Studies," *IEEE Transactions on Automatic Control,* Vol. AC-31, No. 11, 1986,

pp. 995–1014.

[6]Miyazawa, Y., and Dowell, E. H., "Robust Control System Design with Multiple Model Approach and Its Application to Active Flutter Control," *Proceedings of the AIAA Guidance, Navigation, and Control Conference* (Boston, MA), AIAA, Washington, DC, 1989 (AIAA Paper 89-3578).

[7]Nesline, F. W., and Zarchan, P., "Why Modern Controllers Can Go Unstable in Practice," *Journal of Guidance, Control, and Dynamics,* Vol. 7, No. 4, 1984, pp. 495–500.

[8]Miyazawa, Y., "Robust Flight Control System Design with Multiple Model Approach," *Proceedings of the AIAA Guidance, Navigation, and Control Conference* (Portland, OR), AIAA, Washington, DC, 1990 (AIAA Paper 90-3411); *Journal of Guidance, Control, and Dynamics,* Vol. 15, No. 3, 1992, pp. 785–788.

[9]Miyazawa, Y., "Robust Flight-Path Control System Design with Multiple Delay Model Approach," *Proceedings of the AIAA Guidance, Navigation, and Control Conference* (New Orleans, LA), AIAA, Washington, DC, 1991 (AIAA Paper 91-2671).

[10]Stein, G., and Doyle, J. C., "Beyond Singular Values and Loop Shapes," *Journal of Guidance, Control, and Dynamics,* Vol. 14, No. 1, 1991, pp. 5–16.

[11]Bryson, A. E., Jr., and Ho, Y. C., *Applied Optimal Control,* Blaisdell, Waltham, MA, 1969, Chap. 5.

[12]Anderson, B. D. O., and Moore, M. B., *Optimal Control, Linear Quadratic Methods,* Prentice-Hall, Englewood Cliffs, NJ, 1990, Sec. 4.3.

[13]Data Set Handbook of the Dornier Do228-200 Aircraft, BM20-32/88, Dornier GmbH, Friedrichshafen, Germany, 1988.